Supporting information

Activated carbon coated carbon nanotubes for energy storage in supercapacitors and capacitive water purification

Kaiyuan Shi, Meng Ren and Igor Zhitomirsky*

Department of Materials Science and Engineering, McMaster University

1280 Main Street West

Hamilton, Ontario, Canada L8S 4L7

*Phone +1-905-525-9140

*e-mail: zhitom@mcmaster.ca

Pages 17

Figures 13

Tables 1

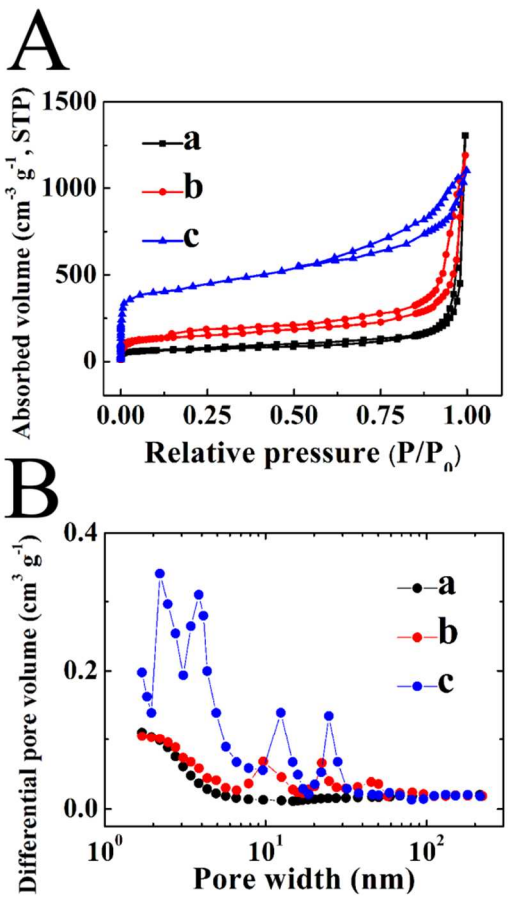

Figure S1. (A) Nitrogen adsorption-desorption isotherms at -196 ˚C and (B) corresponding pore-size distributions calculated with the Barrett-Joyner-Halenda (BJH) method for (a) pristine MWCNT, (b) N-C-MWCNT and (c) N-AC- MWCNT.

In Figure S1A, pristine MWCNT showed an intermediate shape between types II and IV (in the IUPAC classification) with a small hysteresis loop extending from P/P_0= 0.82 to 0.99. For N-C-

MWCNT, there is an increase of N_2 adsorption at high partial pressures indicating increase of pores volume and the hysteresis is also more pronounced than in the pristine tubes. After the chemical activation, the N-AC-MWCNT showed close to type IV dependence with steep uptakes below P/P_0= 0.01 and clear hysteresis loops, which indicated the coexistence of micropores (<2 nm) and mesopores (2~50 nm) in the coating (Figure S1B).

Table S1. Chemical composition from XPS data.

	C (wt %)	O (wt %)	N (wt %)	S (wt %)
Pristine MWCNT	95.57	4.43	-	-
N-AC- MWCNT	83.12	7.89	6.71	2.28

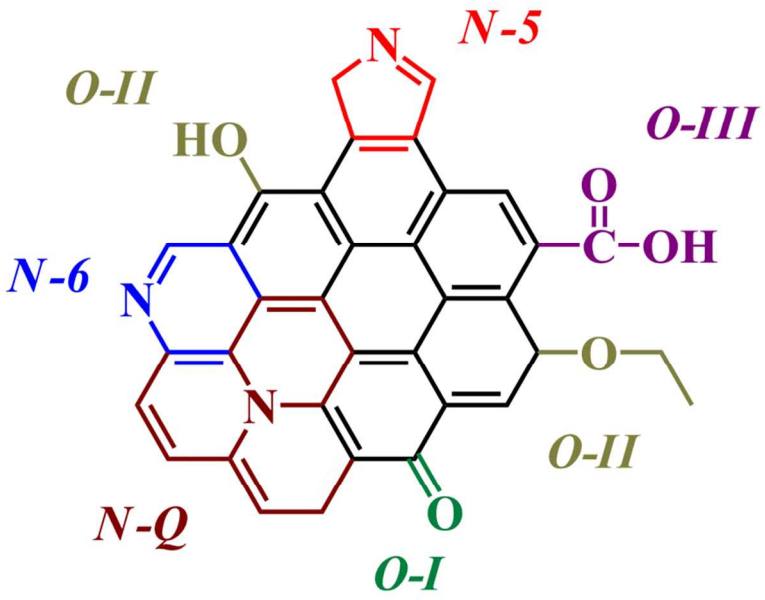

Figure S2. Schematic model of different functional groups in N-AC-MWCNT.

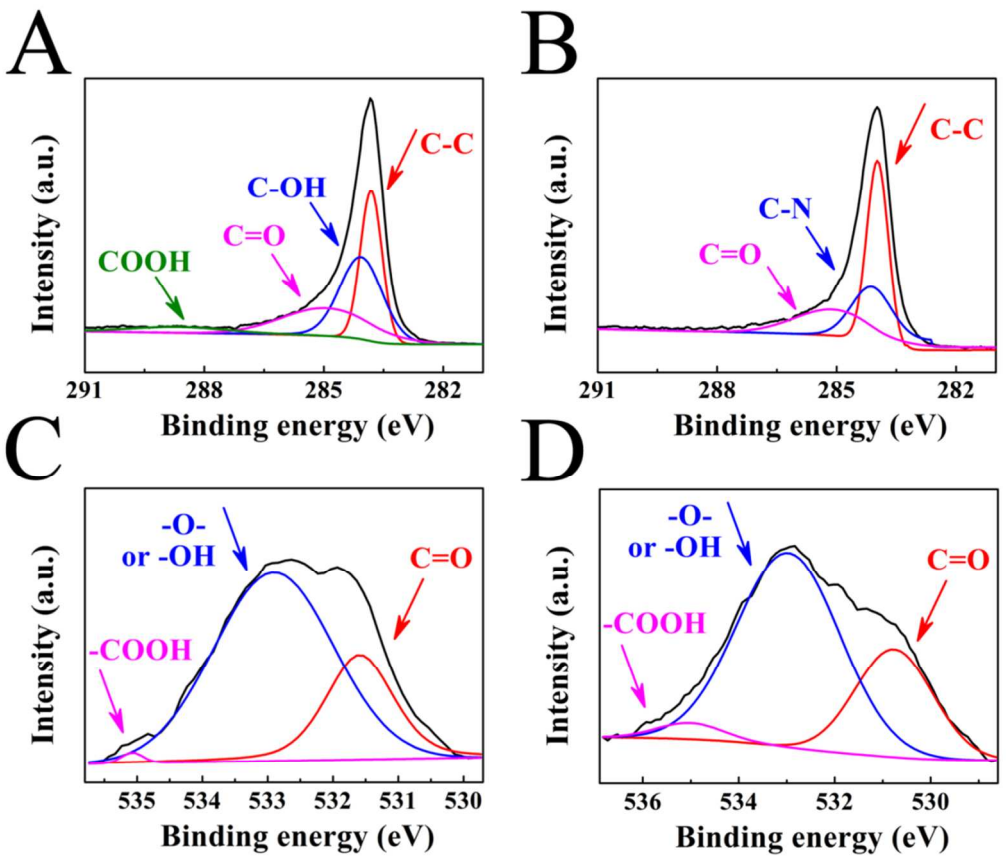

Figure S3. XPS spectra of (A, B) C 1s and (C, D) O 1s; (A, C) pristine MWCNT, (B, D) N-AC-MWCNT.

The high-resolution C1s spectra of MWCNT (Figure S3A) can be fitted by four individual component peaks corresponding to COOH (289.3 eV), C=O (285.8 eV), C-OH (284.6 eV) and C-C (284.2 eV)[1-3]. For N-AC- MWCN (Figure S3B), COOH (289.3 eV) peak disappeared and C-N peak at (284.4 eV) appear. It further confirms that MWCNT was wrapped by N-doped activated carbon. The high-resolution O1s spectrum in Figure S3C and D revealed the existence of several oxygen-based groups including C=O groups (531.2 eV), and C-OH and/or C-C groups (533.1 eV), and COOH groups (535.1 eV).

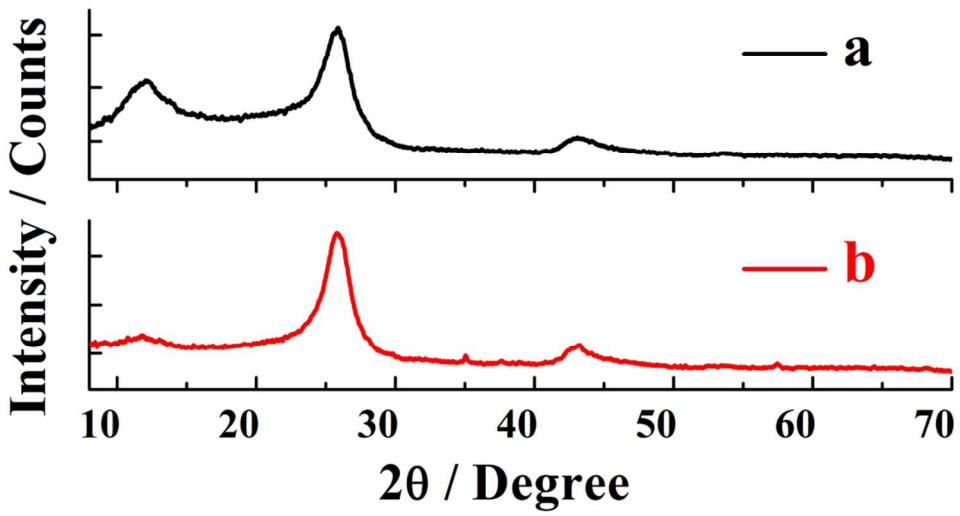

Figure S4. XRD pattern for (a) pristine MWCNT and (b) N-AC-MWCNT.

X-ray diffraction (XRD) studies were performed using Nicolet I2 diffractometer with monochromatized CuK_{α} radiation. The Raman spectroscopy investigations were performed using LabRAM Hr800 instrument. XRD and Raman spectroscopy were carried out to analyze the degrees of carbon graphitization. Figure S4 shows peaks at 25.9˚ and 43.1˚ which can be assigned to (002) and (100) planes of graphite. The broad peak at 11.8˚ is due to amorphous carbon.

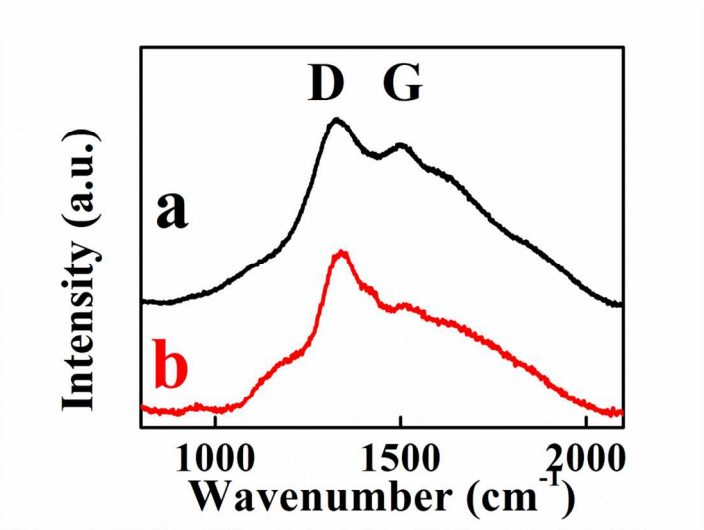

Figure S5 Raman spectrum of (a) pristine MWCNT and (b) N-AC-MWCNT.

The Raman spectrum (Figure S5) clearly indicates the well-known D-band peak at ~1330 cm^{-1} and G-band at ~1520 cm^{-1}. The peak at ~1330 cm^{-1} (D-band) corresponds to the defects and edge planes. The peak at ~1520 cm^{-1} (G-band) can be attributed to the stretching vibration of any pair of sp^2 sites inside the graphitic pattern[4]. The strong D-band peak (Figure S5b) demonstrates that N-AC-MWCNT has a low degree of graphitization and contains a significant amount of disordered sections and defects.

Figure S6. The sedimentation tests for 1 g L^{-1} of (A) pristine MWCNT and (B) N-AC-MWCNT in 0.5 M Na_2SO_4 aqueous electrolyte 30 min after ultrasonication.

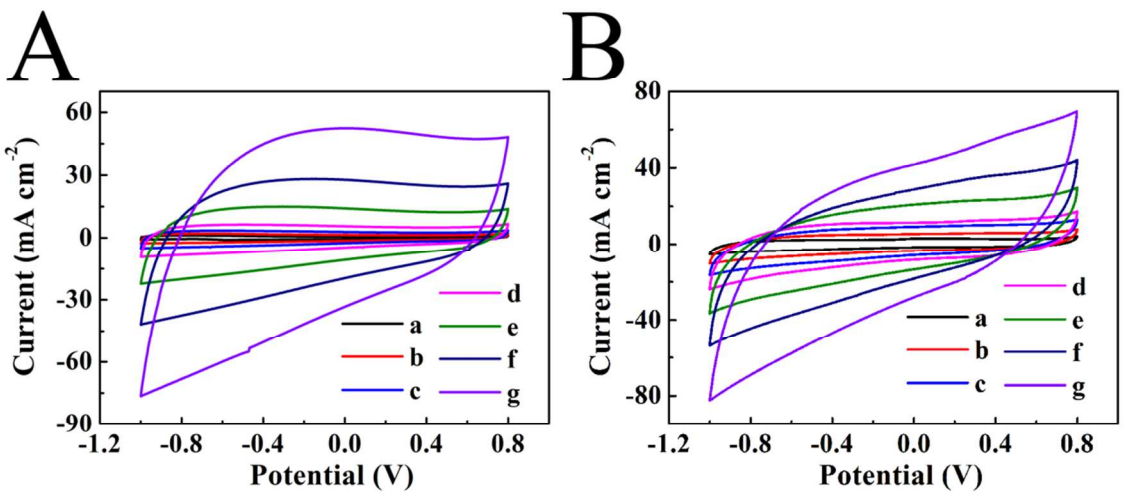

Figure S7. CVs for (A) pristine MWCNT and (B) N-C-MWCNT at the scan rates of (a) 2, (b) 5, (c) 10, (d)20, (e) 50, (f) 100 and (g) 200 mV s^{-1} for electrodes with mass loading of 15 mg cm^{-2}.

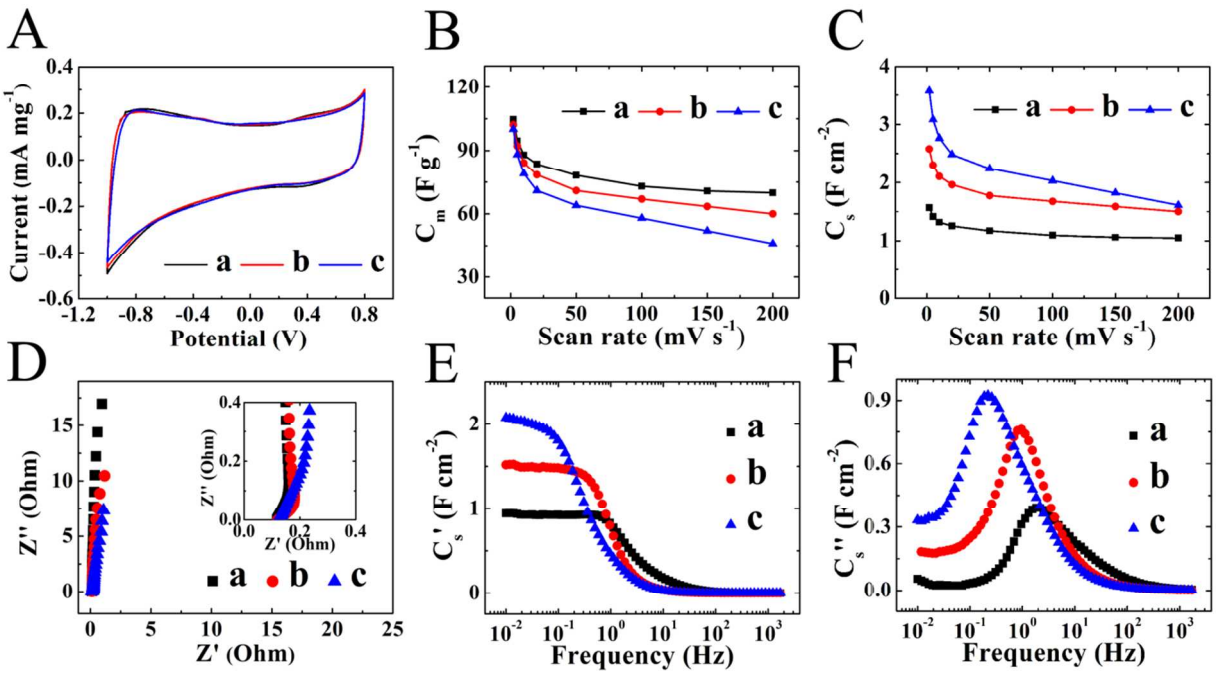

Figure S8. (A) CVs at a scan rate of 5 mV s^{-1}, (B) C_m and (C) C_s obtained from the CV data versus scan rate, (D) Nyquist plots of complex impedance (inset shows high frequency range), (E) C_s' and (F) C_s'' calculated from impedance data versus frequency for N-AC-MWCNT, with a mass loading of (a) 15, (b) 25 and (c) 35 mg cm^{-2}.

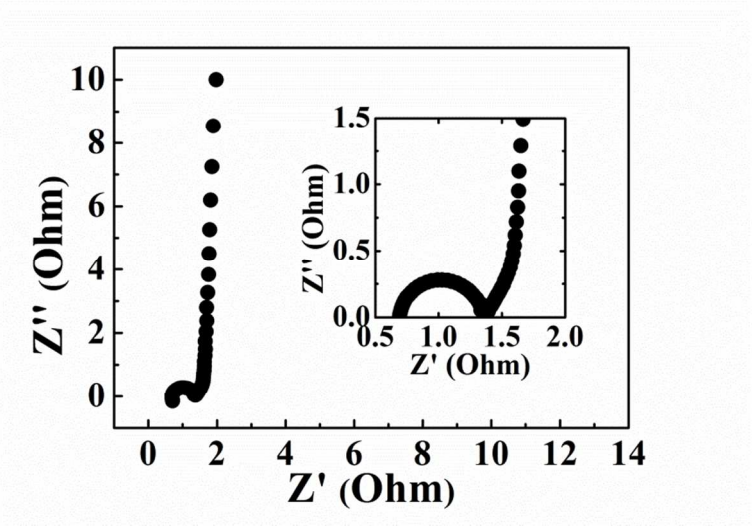

Figure S9. Nyquist plots for a coin cell, containing two N-AC-MWCNT electrodes. Inset shows high frequency range.

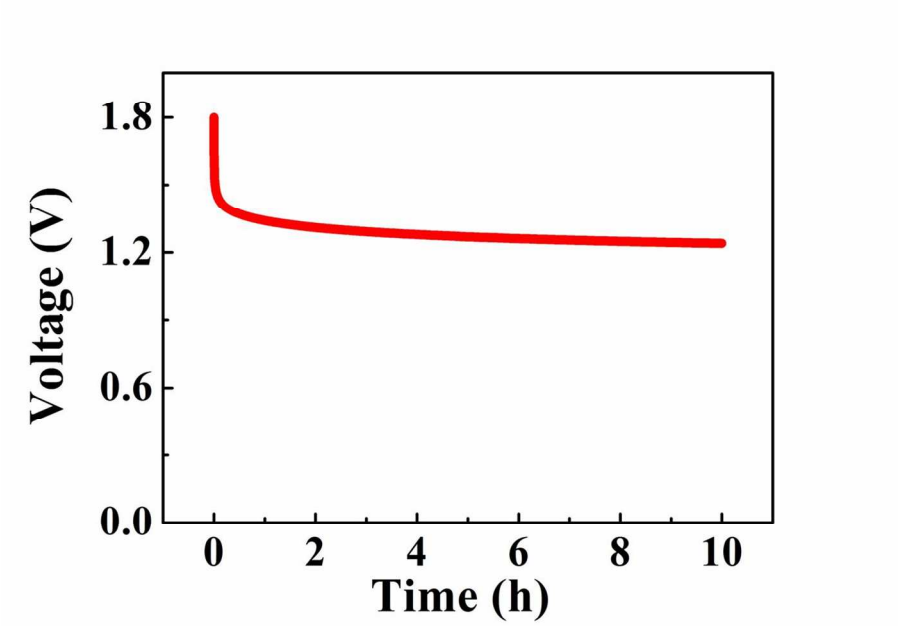

Figure S10. Self discharge test of a coin cell

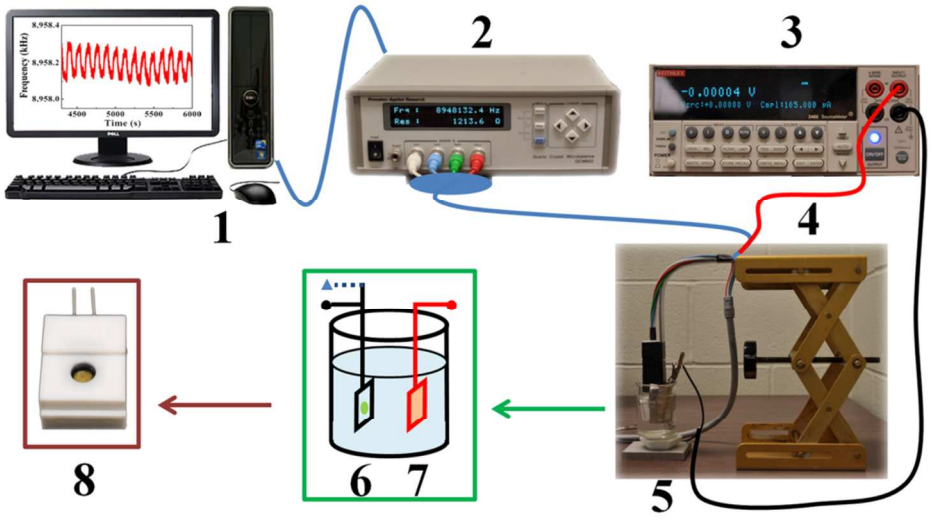

Figure S11. The scheme of experimental setup for analysis of electrosorption and electrodesorption of ions and charged dyes in MWCNT and N-AC-MWCNT deposited on quartz resonators: 1) computer for data collection, 2) quartz-crystal microbalance (QCM), 3) sourcemeter (Keithley Model 2400), 4) support, 5) two electrode measurement cell, containing 6) a working electrode and 7) a platinum foil and 8) 9-MHz Au-coated quartz crystal as a working electrode in a sample holder. The sourcemeter was connected to working electrode and platinum foil. QCM was used to measure the mass variation of the working electrode.

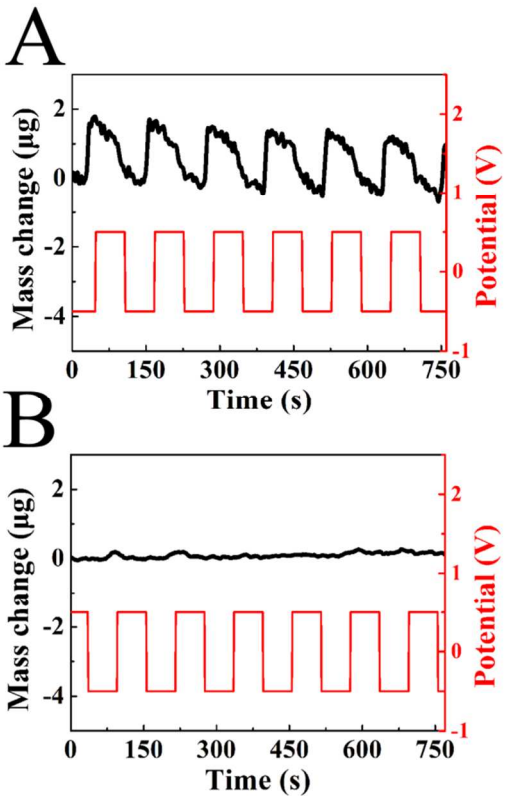

Figure S12. QCM data for mass variation of pristine MWCNT coated resonators during periodic positive and negative pulses with duration of 60 s in (A) 0.05 M Na_2SO_4 and (B) 0.001 M MB dye solutions.

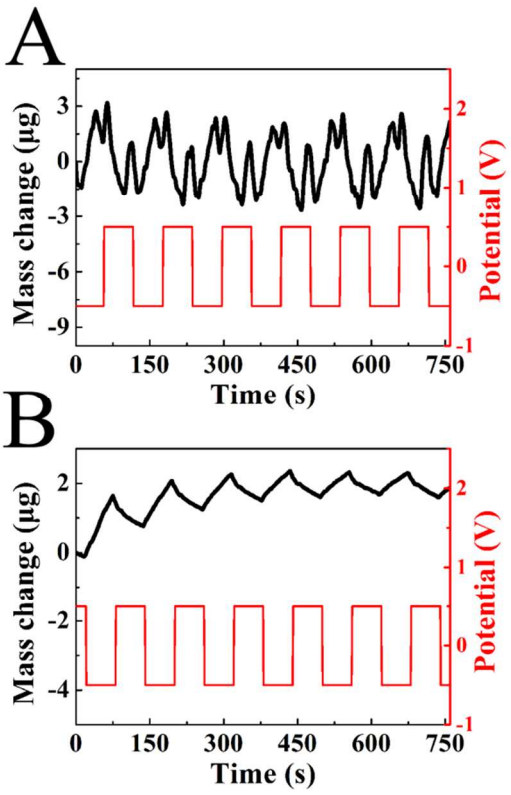

Figure S13. QCM data for mass variation measured in 0.05 M NaCl during periodic positive and negative pulses with duration of 60s for A) N-AC-MWCNT and B) pristine MWCNT coated resonators.

References:

1. Biniak, S.; Szymański, G.; Siedlewski, J.; Świa□tkowski, A., The characterization of activated carbons with oxygen and nitrogen surface groups. *Carbon,* **1997,** 35, (12), 1799-1810.

2. Funabashi, T.; Mizuno, J.; Sato, M.; Kitajima, M.; Matsuura, M.; Shoji, S., Film of lignocellulosic carbon material for self-supporting electrodes in electric double-layer capacitors. *APL Materials,* **2013,** 032104, 1-4.

3. Hulicova-Jurcakova, D.; Seredych, M.; Lu, G. Q.; Bandosz, T. J., Combined Effect of Nitrogen- and Oxygen-Containing Functional Groups of Microporous Activated Carbon on its Electrochemical Performance in Supercapacitors. *Adv. Funct. Mater.,* **2009,** 19, (3), 438-447.

4. Lehman, J. H.; Terrones, M.; Mansfield, E.; Hurst, K. E.; Meunier, V., Evaluating the characteristics of multiwall carbon nanotubes. *Carbon,* **2011,** 49, (8), 2581-2602.